mGluR-Dependent Long-Term Depression Is Associated with Increased Phosphorylation of S6 and Synthesis of Elongation Factor 1A but Remains Expressed in S6K-Deficient Mice[▽]

Marcia D. Antion,[1]† Lingfei Hou,[2,3] Helen Wong,[3] Charles A. Hoeffer,[2,3] and Eric Klann[1,2,3]*

Departments of Neuroscience[1] and Molecular Physiology and Biophysics,[2] Baylor College of Medicine, Houston, Texas 77030, and Center for Neural Science, New York University, New York, New York 10003[3]

Metabotropic glutamate receptor-dependent long-term depression (mGluR-LTD) in the hippocampus requires rapid protein synthesis, which suggests that mGluR activation is coupled to signaling pathways that regulate translation. Herein, we have investigated the signaling pathways that couple group I mGluRs to ribosomal S6 protein phosphorylation and 5′oligopyrimidine tract (5′TOP)-encoded protein synthesis during mGluR-LTD. We found that mGluR-LTD was associated with increased phosphorylation of p70S6 kinase (S6K1) and S6, as well as the synthesis of the 5′TOP-encoded protein elongation factor 1A (EF1A). Moreover, we found that LTD-associated increases in S6K1 phosphorylation, S6 phosphorylation, and levels of EF1A were sensitive to inhibitors of phosphoinositide 3-kinase (PI3K), mammalian target of rapamycin (mTOR), and extracellular signal-regulated kinase (ERK). However, mGluR-LTD was normal in S6K1 knockout mice and enhanced in both S6K2 knockout mice and S6K1/S6K2 double knockout mice. In addition, we observed that LTD-associated increases in S6 phosphorylation were still increased in S6K1- and S6K2-deficient mice, whereas basal levels of EF1A were abnormally elevated. Taken together, these findings indicate that mGluR-LTD is associated with PI3K-, mTOR-, and ERK-dependent alterations in the phosphorylation of S6 and S6K. Our data also suggest that S6Ks are not required for the expression of mGluR-LTD and that the synthesis of 5′TOP-encoded proteins is independent of S6Ks during mGluR-LTD.

The activation of group I metabotropic glutamate receptors (mGluRs) is intimately involved in the regulation of protein synthesis in neurons. Brief application of the mGluR I agonist [3,5-RS] dihydroxyphenylhydrazine (DHPG) has been reported to enhance de novo protein synthesis in hippocampal slices (37) and synaptoneurosomes (12), alter mRNA granule distribution (3), enhance polyribosome formation in synaptoneurosomes (12, 52), and promote rapid dendritic protein synthesis during mGluR-dependent long-term depression (mGluR-LTD) (19). These findings strongly suggest that mGluR-mediated signaling is directly coupled to the regulation of translation initiation in neurons.

Multiple signaling pathways critical for regulating protein synthesis have been reported to be required for mGluR-LTD. Both mammalian target of rapamycin (mTOR) and extracellular signal-regulated kinase (ERK) are activated during mGluR-LTD, and inhibitors of these kinases, as well as inhibitors of phosphoinositide-3-kinase (PI3K), have been shown to block mGluR-LTD (4, 9, 16). Substrates of mTOR and ERK that are known to be involved in translational control during mGluR-LTD include eukaryotic initiation factor 4E and its repressor 4E-binding protein (4). S6 kinases also are known to integrate mTOR, PI3K, and ERK signaling to influence protein synthesis; however, the requirement of S6 kinases for the expression of mGluR-LTD has not been examined.

In mammals, S6 kinases are encoded by two separate genes, S6K1 and S6K2, which are approximately 80% homologous (8). One of the first identified substrates of S6 kinases was ribosomal protein S6, a subunit of the small 40S ribosome. Ribosomal protein S6 is located at the interface of the small and large ribosomal subunits, and evidence suggests that S6 interacts directly with mRNA, tRNA, and translation initiation factors (31). Although the exact consequence of S6 phosphorylation remains unknown, inducible phosphorylation of S6 is often correlated with enhanced cellular growth and protein synthesis (13, 53). Another correlate of enhanced proliferation is selective terminal 5′ oligopyrimidine tract (5′TOP) mRNA translation. A unique feature of 5′TOP mRNAs is that they encode for translation initiation factors and all vertebrate ribosomal protein subunits (28). Synthesis of 5′TOP mRNA-encoded proteins has been observed in dendrites during protein synthesis-dependent long-term potentiation (LTP) parallel to S6K1 activation (49, 50). This suggests that 5′TOP mRNA translation could promote protein synthesis-dependent synaptic plasticity in neurons by improving translational competence in response to the appropriate synaptic signals.

Therefore, we hypothesized that mGluR-LTD would be associated with increased phosphorylation of S6 kinases on sites phosphorylated by ERK and/or mTOR, resulting in the subsequent phosphorylation of S6 and translation of 5′TOP mRNAs. In these studies, we measured the phosphorylation of p70S6K (the dominant cytoplasmic S6 kinase derived from S6K1), the phosphorylation of ribosomal protein S6, and the levels of several 5′TOP-encoded proteins, including elongation

* Corresponding author. Mailing address: Center for Neural Science, New York University, 4 Washington Place, Room 809, New York, NY 10003. Phone: (212) 992-9769. Fax: (212) 995-4011. E-mail: eklann@cns.nyu.edu.
† Present address: Department of Physiology, Northwestern University School of Medicine, Ward 7-275, 303 E. Chicago Ave., Chicago, IL 60611.

factor 1A (EF1A) and S6 itself, following mGluR-LTD induction. In addition, we asked whether S6 kinases are required for the normal expression of mGluR-LTD and synthesis of 5′TOP-encoded proteins. Our findings indicate that the activation of ERK, PI3K, and mTOR associated with mGluR-LTD is correlated with increases in the phosphorylation of S6K1 and S6 ribosomal protein and an elevation in the levels of the 5′TOP-encoded protein EF1A. Surprisingly, we found that the genetic removal of S6K1 and/or S6K2 did not block mGluR-LTD; rather, we observed altered expression of LTD that was accompanied by abnormal levels of EF1A in the S6K mutant mice. Taken together, we find that multiple kinase signaling pathways interact to modulate the translation of 5′TOP mRNAs during mGluR-LTD.

MATERIALS AND METHODS

Materials. The following chemicals were obtained from the respective companies: DHPG, UO126, and LY365354 from Tocris Cookson, Ellisville, MO; wortmannin and LY294002 from Alexis Corporation, Carlsbad, CA; ascomycin, anisomycin, MG132, and SL-327 from Sigma, St. Louis, MO; and rapamycin from Cell Signaling Technology, Beverly, MA. MPEP [2-methyl-6-(phenylethynyl)-pyridine] was a gift from the FRAXA Foundation to E. Klann. I-Block was obtained from Tropix (Bedford, MA). All antibodies were obtained from Cell Signaling Technology with the exception of the following: EF1A (EF-Tu) from Chemicon, Temecula, CA; ERK from Promega, Madison, WI; and p70S6K (C-18) from Santa Cruz Biotechnology, Santa Cruz, CA. Enhanced chemiluminescence kits were obtained from EM Biosciences, Inc. (San Diego, CA), and West-Femto SuperSignal from Pierce Biotechnology, Inc. (Rockford, IL).

Animals. There are two genes that encode for S6 kinases: S6K1 and S6K2 (24, 36, 45). Knockout mice for each of these genes were generously provided by Sara Kozma and George Thomas (University of Cincinnati) and the Novartis Foundation (Basel, Switzerland). These mice were outcrossed one generation to C57BL/6J mice, and the resulting heterozygotes were mated to one another to generate wild-type and knockout littermates. Double heterozygous mice ($S6K1^{+/-}$ $S6K2^{+/-}$) were similarly crossed; however, we were unable to obtain any double knockout ($S6K1^{-/-}$ $S6K2^{-/-}$) mice with this breeding strategy, consistent with previous findings that viable double knockout mice are observed with a frequency of approximately 1:500 (36). To obtain double knockout mice, we crossed $S6K1^{-/-}$ $S6K2^{+/-}$ and $S6K1^{+/-}$ $S6K2^{-/-}$ mice. For studies of the double knockout mice, we used the single knockout littermates resulting from these crosses, as well as age- and strain-matched wild-type mice, as controls. Mice were genotyped before and after completion of experiments via PCR of DNA purified from tail digests with methods previously described (36).

The mice were treated in accordance with the institutional animal care and use committee guidelines at Baylor College of Medicine Center for Comparative Medicine. The animals were given water and food ad libitum and maintained on a 12-h light-dark cycle. C57BL/6 mice were obtained from either Charles River or the Jackson Laboratory and were ordered to arrive at our facility at 3 weeks of age. All animals were used at the age of 4 to 5 weeks for the experiments described.

Preparation and treatment of hippocampal slices. Mice were euthanized by cervical dislocation, and the brain was rapidly removed and suspended into ice-cold sucrose solution containing 110 mM sucrose, 60 mM NaCl, 3 mM KCl, 1.25 mM NaH$_2$PO$_4$, 28 mM NaHCO$_3$, 5 mM glucose, 0.6 mM ascorbic acid, 7 mM MgCl$_2$, and 0.5 mM CaCl$_2$ gassed with 95% O$_2$-5% CO$_2$. The hippocampus was removed and sectioned with a McIllwain tissue chopper, which yielded approximately 15 to 18 hippocampal slices containing well-defined laminated architecture. Slices then were equilibrated for 30 min in 50% ice-cold sucrose solution mixed with 50% ACSF containing 125 mM NaCl, 2.5 mM KCl, 1.25 mM NaH$_2$PO$_4$, 25 mM NaHCO$_3$, 25 mM glucose, 1 mM MgCl$_2$, and 2 mM CaCl$_2$ gassed with 95% O$_2$-5% CO$_2$. Slices then were incubated for at least 1 h at room temperature in 100% ACSF. Hippocampal slices were divided into five to six groups containing three to four slices and equilibrated for 2 h at 32°C in 100% ACSF prior to treatment. DHPG was suspended into a 5 mM stock solution in ACSF each experimental day, and slices were treated with a final concentration of 50 μM for 10 min prior to being snap-frozen over dry ice. Inhibitors were added 30 min to 1 h prior to DHPG application. In some cases, inhibitors were suspended in methanol or dimethyl sulfoxide (DMSO). In these instances, all slices within the experiment were treated with the same amount of vehicle. DMSO never exceeded more than 0.01% and methanol 0.05% of the total

solution volume in which hippocampal slices were exposed. Frozen slices were briefly thawed for microdissection of area CA1 and then suspended into 45 μl of ice-cold buffer containing 10 mM HEPES, 150 mM NaCl, 1 mM EDTA, 1 mM EGTA, 10 mM Na$_4$P$_2$O$_7$, and 10 μl/ml of each of the following inhibitors: protease inhibitor cocktail 1, phosphatase inhibitor cocktail 1, and phosphatase inhibitor cocktail 2 (Sigma, St. Louis, MO). After brief sonication, samples were centrifuged at 1,000 × g for 5 s to remove debris and the supernatant was used for the experiments described.

Western blots. Protein samples were dissolved in 3× sample buffer on ice to achieve a final concentration of 0.75 to 1.5 μg/μl. Ten micrograms of protein was resolved via sodium dodecyl sulfate-polyacrylamide gel electrophoresis and blotted onto polyvinylidene fluoride membranes in a methanol-based Tris-glycine buffer at 4°C and 650 mA for 6 h. Membranes then were dried briefly at room temperature to resolve by eye the blotted bands and carefully cut into strips using a broad-range molecular weight marker (Bio-Rad, Hercules, CA) as a guide for each protein to be probed. Each primary antibody was suspended into 0.2% I-Block in Tween–Tris-buffered saline (TTBS) (0.1% Tween 20) in a total volume of 5 to 10 ml and incubated over the membrane with vigorous mixing either 2 h at room temperature or overnight at 4°C. Primary antibodies included Ser235/Ser236 S6 (1:1,000), Ser240/Ser244 S6, monoclonal rabbit 5G10 (1:750), EF1A (1:50,000), Thr185/Tyr187 ERK (1:5,000), ERK (1:10,000), Ser2448 mTOR (1:1,000), mTOR (1:1,000), polyclonal rabbit Thr389 S6K1 (1:750), Thr421/Ser424 S6K1 (1:1,000), and S6K1 (1:1,000 [Cell Signaling] or 1:200 [C-18; Santa Cruz]). Membranes were rinsed at least three times in TTBS, 5 min each, and incubated in secondary antibody conjugated to horseradish peroxidase (1:5,000) in I-Block for 1 to 2 h more at room temperature. After a final set of TTBS rinses, membranes were suspended in enhanced chemiluminescence fluid for 1 to 5 min and exposed to Kodak Xomat film for 30 s to 10 min. Membranes were stripped in a 2 mM glycine, 2% sodium dodecyl sulfate, pH 2.0, solution at 55°C with vigorous shaking for 1 to 2 h, rinsed in TBS, and reprobed with another antibody. Blots were analyzed using Scion Image densitometry (Scion, Frederick, MD). A Student t test was performed between treated groups and their controls. A one-way analysis of variance (ANOVA) was conducted where multiple comparisons within experiments were measured, followed by a Tukey test where appropriate. For each figure, a P value of <0.05 was considered statistically significant and a P value of <0.1 but >0.05 was considered a statistical trend.

mTOR activity assay. Hippocampal slices were treated with DHPG (50 μM for 10 min) or untreated, flash frozen on dry ice, and homogenized in assay buffer according to the K-LISA mTOR activity kit manufacturer's directions (EMD-Calbiochem, San Diego, CA). mTOR was purified from 60 μg of the hippocampal homogenate with a 2-h, 4°C incubation with mTOR antibody (1:100; Cell Signaling, Beverly, MA) followed by immunoprecipitation with Protein-G Plus beads (Pierce, Rockford, IL). The resultant mTOR extract was assayed according to the K-LISA mTOR activity kit manufacturer's instructions. mTOR activity was measured by enzyme-linked immunosorbent assay with the substrate absorbance measured at 450 nm and reference wavelengths measured at 540/595 nm with a Synergy 2 multidetection microplate reader (BioTek).

Immunohistochemistry. Sections of 400 μm were treated with DHPG or untreated as described above and immediately fixed in ice-cold 4% paraformaldehyde-1% glutaraldehyde solution in 0.1 M phosphate-buffered saline (PBS), pH 7.4, containing 2 mM NaF and 2 mM Na$_3$VO$_4$ overnight at 4°C. Sections were rinsed in 30% sucrose in PBS until they precipitated over approximately 3 nights at 4°C. Sections then were embedded in O.C.T. compound (VWR) over dry ice and stored at −80°C until they were sectioned at 20 μm with a cryostat. Floating sections were rinsed in PBS and then PBS containing 0.7% Triton-X (PBSX) before being placed into 10% normal goat serum in PBSX overnight at 4°C. Primary-antibody dilutions were as follows: Ser235/236 S6 at 1:200 and EF1A at 1:1,000. Sections were incubated in primary antibody with gentle shaking overnight at 4°C, rinsed five times in PBSX, and then incubated in Cy3-conjugated secondary antibody (1:500) for 2 h at room temperature with gentle shaking. Sections were imaged using a Zeiss 510 meta confocal microscope system (Zeiss, Oberkochen, Germany). For analysis, images were subdivided into discrete compartments 20 μm long by 5 μm across from the interface of the stratum pyramidale and stratum radiatum. The numbers of pixels highlighted were averaged together across similar compartments for the total number of slices.

Electrophysiology. Hippocampal slices were isolated as described above. Slices were incubated at 30°C within a humidified interface chamber (Fine Science Tools, North Vancouver, BC, Canada) perfused with oxygenated ACSF at a rate of 1 ml/min. In most cases, field excitatory postsynaptic potentials (fEPSPs) in slices from wild-type and knockout mice were recorded at the same time. A dual recording amplifier (A&M Systems, Sequim, WA) was interfaced to two glass micropipette recording electrodes filled with ACSF with an approximate resistance of 1 to 5 MΩ. Slices were each stimulated via a stimulus isolator (A&M
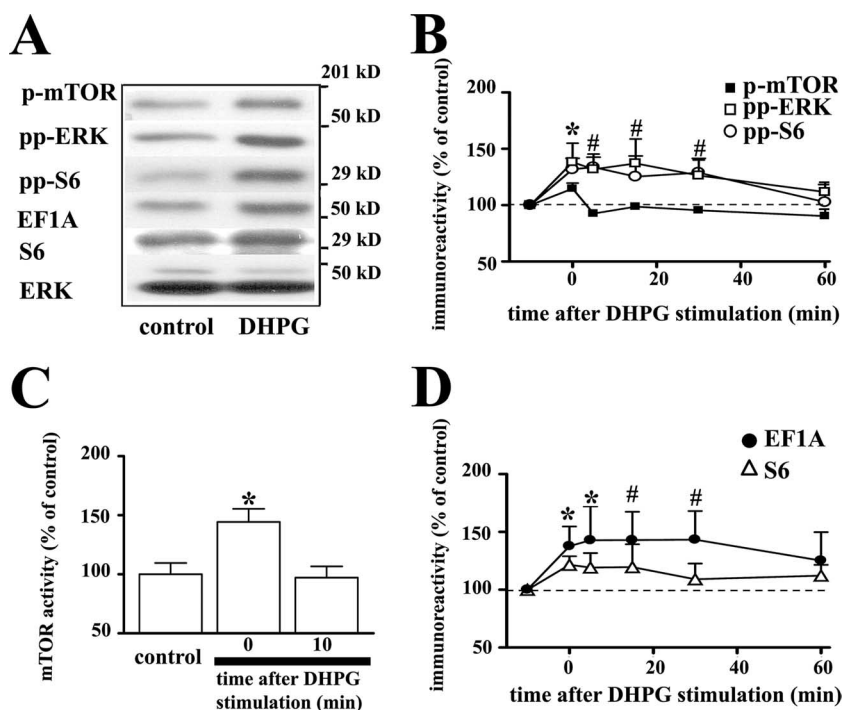
FIG. 1. mGluR-LTD is associated with transient phosphorylation of mTOR, ERK, and ribosomal protein S6 in hippocampal area CA1 that is accompanied by enhanced synthesis of the 5′TOP-encoded proteins EF1A and S6. Hippocampal slices were exposed to DHPG (50 μM) for 10 min and incubated in ACSF for the indicated times. (A) Representative Western blots from the same experiment for phosphorylated mTOR (p-mTOR), phosphorylated ERK (pp-ERK), phosphorylated S6 (pp-S6), EF1A, total S6 (S6), and total ERK (ERK) from untreated (control) and DHPG-treated slices. Numbers on the right indicate molecular size markers. (B and D) After DHPG stimulation, slices were harvested immediately after treatment (0 min) and 5, 15, 30, and 60 min thereafter. Immunoreactivity was normalized to total ERK and graphed as percent control. Values are means ± standard errors of the means determined immediately after DHPG stimulation. (B) Percentages of control values are as follows: for pp-S6 with DHPG, 132% ± 10% ($n = 7$); for p-mTOR with DHPG, 115% ± 5% ($n = 5$); and for pp-ERK with DHPG, 138% ± 17% ($n = 5$). *, statistical significance above control for all groups; #, statistical significance above control for pp-ERK. (C) After DHPG stimulation, slices were assayed immediately (0 min) or 10 min later for mTOR phosphotransferase activity. Percentages of control values are as follows: for mTOR activity with DHPG (0 min), 144% ± 11% ($n = 7$), and for DHPG (10 min), 97% ± 9% ($n = 5$). *, statistical significance above control mTOR activity levels. (D) Percentage of control EF1A value for DHPG is 122% ± 7% ($n = 7$), and percentage of control value for total S6 values with DHPG is 138% ± 17% ($n = 3$). *, statistical significance above control for all groups; #, statistical significance above control for S6.

Systems) within the range of 0 to 1.5 mV intensity, a frequency of 0.05 Hz, and a total duration of 0.05 ms. Bipolar stimulating electrodes were handmade with isonel-coated platinum (thickness of approximately 0.5 mm) and delicately placed onto the Schaffer collaterals of each slice. Recording electrodes were placed into the stratum radiatum, and the signal was converted into a digital signal via a Digidata 1322 model interface (A&M Systems). Patchclamp version 8.2 software was configured to collect the signal. Each trace was averaged over a period of 2 min, and the initial slope (approximately 0.2 to 0.3 ms following the cessation of the fiber volley) was selected. For each slice, an input-output curve was generated, and test pulses for recordings were selected to yield a 50 to 60% maximal fEPSP slope, which yielded a trace of approximately 1 to 6 mV in amplitude. Baseline recordings were taken for a minimum of 20 min prior to treatment. Data were expressed as a percentage of the baseline recording prior to treatment. A two-way ANOVA was performed on the data with genotype X interaction as the reported F value, post hoc Bonferonni tests were done where appropriate, and a P value of <0.05 was considered statistically significant.

RESULTS

Phosphorylation of S6 and synthesis of two species of 5′TOP-encoded proteins are associated with mGluR-LTD. Brief application of DHPG has been reported to induce mGluR-LTD that is associated with the activation of mTOR and ERK2 (4, 9, 16, 39). We confirmed that the phosphoryla-

tion of both mTOR and ERK2 was increased during DHPG-induced mGluR-LTD (Fig. 1A and B). We observed that the increase in mTOR phosphorylation was followed by a rapid dephosphorylation after washout of DHPG, whereas phosphorylated ERK2 remained significantly elevated up to 30 min following washout of DHPG (Fig. 1B). To confirm that the LTD-associated increase in the phosphorylation of mTOR correlated with increased enzymatic activity during mGluR-LTD, we performed an immunocomplex assay to measure the phosphotransferase activity of mTOR. We observed that mTOR activity was transiently elevated in slices treated with DHPG with a time scale similar to that of the phosphorylation (Fig. 1C). Within the same set of experiments, we observed that mGluR-LTD triggered an increase in the phosphorylation of ribosomal protein S6 that persisted up to 30 min following DHPG washout (Fig. 1A and B). We next asked whether mGluR-LTD was associated with an increase in the synthesis of the 5′TOP-encoded proteins EF1A and S6 itself. We observed that EF1A and S6 levels were enhanced immediately after DHPG treatment and remained elevated 15 to 30 min after washout of DHPG (Fig. 1A and D). To test whether the
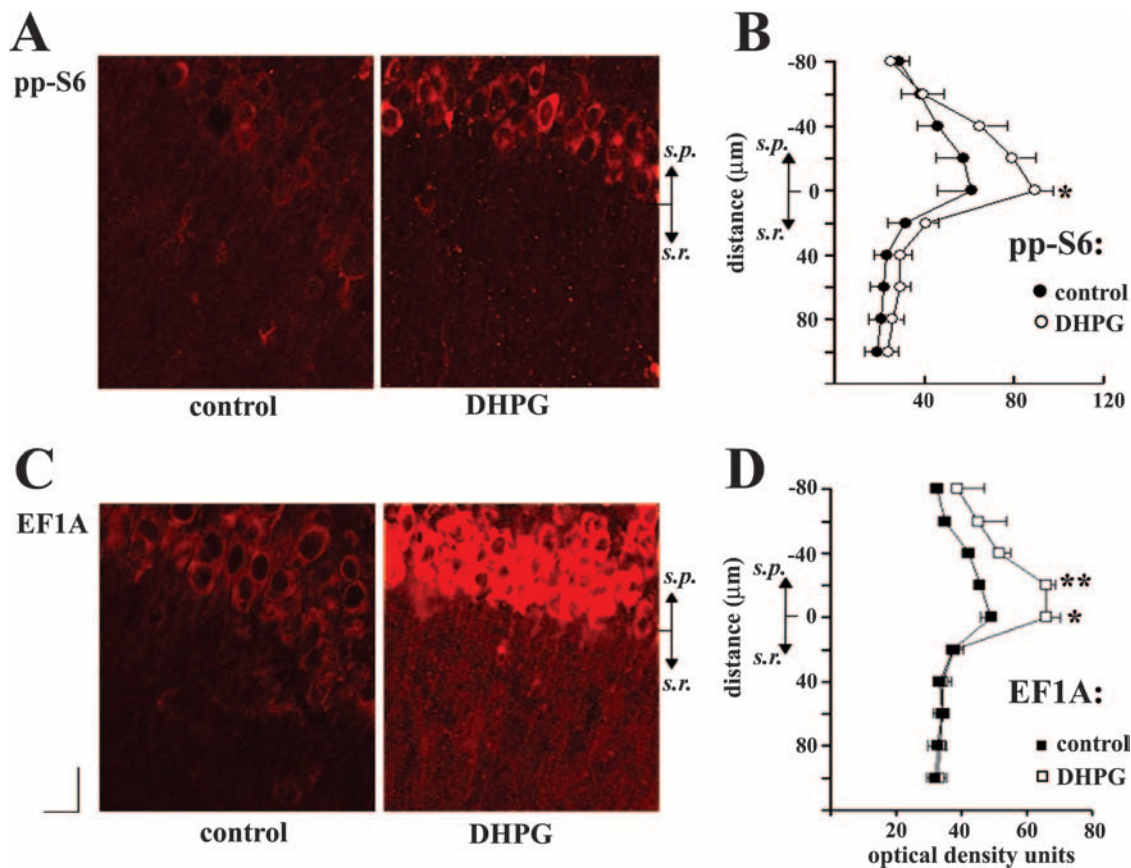
FIG. 2. mGluR-LTD is associated with increased phosphorylated S6 and EF1A levels in area CA1. Representative confocal images in soma and dendrites of hippocampal area CA1 from DHPG-treated and untreated slices (control). To determine whether there was elevated immunoreactivity in the dendrites and/or the soma of area CA1, the optical densities of the images were quantified in 20-μm intervals from the interface of the stratum pyramidale (s.p.) and stratum radiatum (s.r.) in control and DHPG-treated slices for pp-S6 ($n = 4$) and EF1A ($n = 4$). Elevations of pp-S6 and EF1A levels were detected in the s.p. but not in the s.r. with this method. Statistics were computed with a two-way ANOVA; post hoc Bonferroni t tests revealed significance (∗, $P < 0.05$; ∗∗, $P < 0.001$). Images were taken with a 20× objective. Bar, 20 μm.

DHPG-induced elevation of EF1A and S6 resulted from enhanced protein synthesis, we pretreated slices for 20 min in the presence of 40 μM anisomycin. We found that anisomycin treatment abrogated the elevation of EF1A (percentages of control EF1A values were 114% ± 5% for DHPG [$P < 0.05$] and 83% ± 17% for DHPG plus anisomycin [$n = 4$]) and S6 (percentages of control S6 values were 128% ± 10% for DHPG [$P < 0.05$] and 81% ± 6% for DHPG plus anisomycin [$n = 4$]). We also examined whether decreased protein degradation contributed to the increases in EF1A and S6 associated with LTD. We found that pretreatment of slices with the proteasome inhibitor MG132 (20 μM) for 20 min altered neither the basal levels nor the DHPG-induced increase in the levels of EF1A and S6 (data not shown). Together these findings support the hypothesis that de novo protein synthesis from 5′TOP mRNA is associated with mGluR-LTD.

To examine whether the increases in phosphorylated S6 and EF1A levels were expressed in specific subcellular compartments during mGluR-LTD, we utilized immunohistochemical labeling. We observed that phosphorylated S6 and EF1A shared similar distributions. Noticeably, for both phosphorylated S6 and EF1A, the somatic region was prominently labeled in comparison to the modest signal detected in the den-

drites of stratum radiatum (Fig. 2A and B). Staining of interleaved slices treated with DHPG revealed a modest increase in signal for phosphorylated S6 (Fig. 2A) and a dramatic elevation of EF1A levels (Fig. 2C) in area CA1. To determine whether the elevated staining intensity was compartmentalized to either dendritic or somatic regions of CA1, we quantified the optical density of each interleaved pair of slices at discrete intervals. We found that the density of phosphorylated S6 and EF1A immunoreactivity was significantly elevated in the somatic layer of CA1. In contrast, we were unable to measure a difference with this immunolabeling method for phosphorylated S6 or EF1A in the stratum radiatum. We also observed that the initial compact layer of stratum pyramidale neurons interfacing the stratum radiatum exhibited enhanced intensity compared to those stratum pyramidale neurons neighboring the stratum oriens. These findings demonstrate that mGluR-LTD is associated with increased S6 phosphorylation that is correlated with the elevation of the 5′TOP-encoded protein EF1A primarily in the somatic region of area CA1.

Increased phosphorylation of S6 and enhanced levels of EF1A following mGluR-LTD require both mGluR1 and mGluR5. It previously was reported that the activation of mTOR and
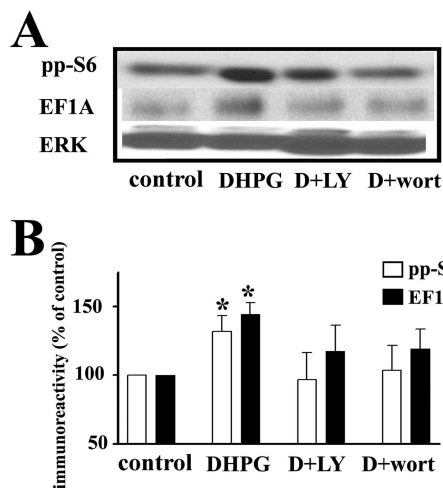
FIG. 3. mGluR-LTD is associated with a PI3K-dependent increase in the levels of phosphorylated ribosomal protein S6 and total levels of the 5′TOP-encoded protein EF1A. Hippocampal slices were incubated in vehicle (0.001% DMSO plus 0.01% methanol), LY292002 (LY) (50 μM), or wortmannin (wort) (100 nm) for 30 min and were then exposed to DHPG (50 μM) for 10 min in the presence of either vehicle (control) or the respective antagonists. (A) Representative Western blots for phosphorylated S6 (pp-S6), EF1A, and total ERK. (B) Immunoreactivity was normalized to total ERK immunoreactivity. Values are means ± standard errors of the means and are expressed as percentages of control values. pp-S6 values are as follows: with DHPG, 132% ± 11% ($n = 8$); with DHPG plus LY (D+LY), 97% ± 20% ($n = 8$); and with DHPG plus wort (D+wort), 103% ± 18% ($n = 5$) (data not shown: with LY, 97% ± 10% [$n = 8$]; with wort, 110% ± 16% [$n = 5$]). EF1A values are as follows: with DHPG, 144% ± 9% ($n = 4$); with DHPG plus LY, 118% ± 19% ($n = 4$); and with DHPG plus wort, 119% ± 15% ($n = 4$) (data not shown: with LY, 120% ± 14% [$n = 4$]; with wort, 97% ± 14% [$n = 4$]). *, statistical significance with a Student t test ($P < 0.05$).

ERK2 associated with mGluR-LTD requires both mGluR1 and mGluR5 (4, 16). Therefore, we determined whether both subtypes of group I mGluRs also contribute to the phosphorylation of S6 and the elevation in EF1A levels that accompany mGluR-LTD. We found that both LY365367 (100 μM, 30 min) and MPEP (10 μM, 30 min), which antagonize mGluR1 and mGluR5, respectively, were able to block the DHPG-induced increase in EF1A (percentages of control EF1A values were 118% ± 4% for DHPG [$P < 0.05$], 104% ± 10% for DHPG plus LY365367, and 106% ± 11% for DHPG plus MPEP [$n = 5$]). In contrast, LY365367, but not MPEP, partially blocked S6 phosphorylation (percentages of control pp-S6 values were 132% ± 9% for DHPG [$P < 0.05$ compared to control], 125% ± 12% for DHPG plus LY365367 [$P < 0.05$ compared to control and $P < 0.05$ compared to DHPG], and 138% ± 15% for DHPG plus MPEP [$P < 0.05$ compared to control] [$n = 5$]). Concomitant application of MPEP and LY365367 completely blocked the LTD-associated increase in S6 phosphorylation and EF1A levels (percentage of control pp-S6 was 113% ± 17% for DHPG plus LY365367 plus MPEP [$n = 4$] and percentage of control EF1A was 88% ± 26% for DHPG plus LY365367 plus MPEP [$n = 3$]). These findings indicate that both mGluR1 and mGluR5 contribute to the increases in S6 phosphorylation and EF1A levels that are associated with mGluR-LTD.
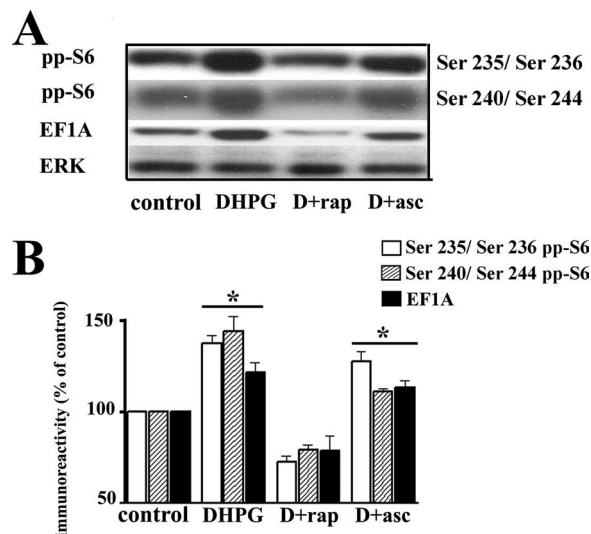

FIG. 4. mGluR-LTD is associated with mTOR-dependent increases in the levels of phosphorylated ribosomal protein S6 and total levels of EF1A. Hippocampal slices were incubated in vehicle (0.01% methanol), rapamycin (rap) (20 nM), a selective antagonist for mTOR, or ascomycin (asc) (20 nM), a molecule structurally similar to rapamycin that does not interfere with mTOR activity, for 30 min and were then exposed to DHPG (50 μM) for 10 min in the presence of vehicle (control) or the respective antagonists. (A) Representative Western blots for S6 phosphorylated at Ser235/Ser236 and Ser240/Ser244 (pp-S6), EF1A, and total ERK. (B) Immunoreactivity was normalized to total ERK immunoreactivity. Values are means ± standard errors of the means and are expressed as percentages of control values. Ser235/Ser236 pp-S6 values are as follows: with DHPG, 138% ± 10% ($n = 6$); with DHPG plus rap (D+rap), 73% ± 8% ($n = 5$); and with DHPG plus asc (D+asc), 128% ± 13% ($n = 5$) (data not shown: with rap, 91% ± 6% [$n = 4$]; with asc, 92% ± 8% [$n = 4$]). Ser240/Ser244 pp-S6 values are as follows: with DHPG, 144% ± 15% ($n = 4$); with DHPG plus rap, 80% ± 5% ($n = 3$); and with DHPG plus asc, 111% ± 2% ($n = 3$) (data not shown: with rap, 89% ± 1% [$n = 2$]; with asc, 89% ± 8% [$n = 2$]). EF1A values are as follows: with DHPG, 122% ± 11% ($n = 4$); with DHPG plus rap, 79% ± 16% ($n = 4$); and with DHPG plus asc, 113% ± 7% ($n = 4$) (data not shown: with rap, 79% ± 23% [$n = 4$]; with asc, 86% ± 28% [$n = 4$]). *, statistical significance with control via Student's t test ($P < 0.05$).

LTD-associated increases in S6 phosphorylation and EF1A protein levels require PI3K, mTOR, and ERK. It previously was reported that PI3K, mTOR, and ERK are necessary for the expression of protein synthesis-dependent mGluR-LTD (4, 9, 16). Therefore, we asked whether increases in phosphorylated S6 and EF1A levels associated with mGluR-LTD required each of these kinases. Inhibition of PI3K with either 50 μM LY292004 or 100 nM wortmannin abrogated the LTD-associated increase in Ser235/Ser236 S6 phosphorylation and the increased synthesis of EF1A (Fig. 3A and B). Similarly, inhibition of mTOR with 20 nM rapamycin abolished the LTD-induced increase in Ser235/Ser236 S6 phosphorylation and the increased expression of EF1A (Fig. 4A and B). We also examined the phosphorylation of the Ser240/Ser244 sites on S6, which have been reported to be regulated more specifically by mTOR-dependent signaling (36, 41). We observed an increase in Ser240/Ser244 S6 phosphorylation following DHPG treatment that was prevented by rapamycin (Fig. 4A and B). The ability of rapamycin to block both the LTD-
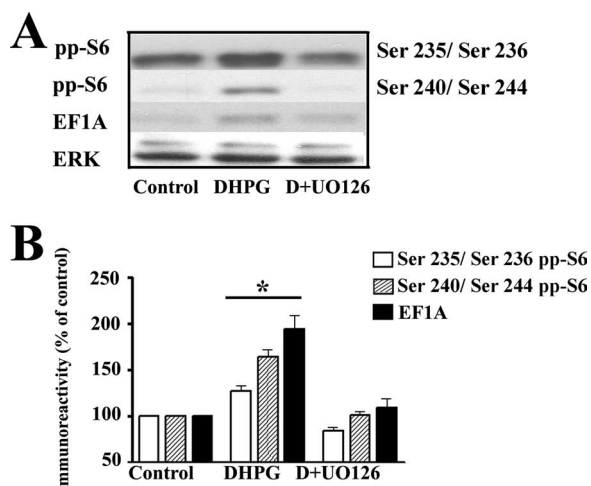
FIG. 5. mGluR-LTD is associated with an ERK-dependent increase in the levels of phosphorylated ribosomal protein S6 and total levels of EF1A. Hippocampal slices were incubated in vehicle (0.01% DMSO), UO126 (20 μM), a selective antagonist for the ERK1/2-specific MEK, or SL327 (5 μM), a structurally distinct antagonist from UO126 for the ERK1/2-specific MEK, for 60 min and were then exposed to DHPG (50 μM) for 10 min in the presence of vehicle (control) or the respective antagonists. (A) Representative Western blots for S6 phosphorylated at Ser235/Ser236 and Ser240/Ser244 (pp-S6), EF1A, and ERK. (B) Immunoreactivity was normalized to total ERK immunoreactivity. Values are means ± standard errors of the means and are expressed as percentages of control values. Ser235/Ser236 pp-S6 values are as follows: with DHPG, 127% ± 14% ($n = 7$), and with DHPG plus UO126 (D+UO126), 84% ± 9% ($n = 7$) (data not shown: with UO126, 90% ± 13% [$n = 6$]; with DHPG plus SL327, 90% ± 4% [$n = 4$]; with SL327, 99% ± 8% [$n = 4$]). Ser240/Ser244 pp-S6 values are as follows: with DHPG, 164% ± 15% ($n = 4$), and with DHPG plus UO126, 101% ± 8% ($n = 4$) (data not shown: with UO126, 91% ± 15% [$n = 4$]; with DHPG plus SL327, 92% ± 8% [$n = 4$]; with SL327, 99% ± 5% [$n = 4$]). EF1A values are as follows: with DHPG, 194% ± 31% ($n = 4$), and with DHPG plus UO126, 109% ± 20% ($n = 4$) (data not shown: with UO126, 120% ± 26% [$n = 4$]; with DHPG plus SL327, 137% ± 50% [$n = 4$]; with SL327, 115% ± 31% [$n = 4$]). *, statistical significance with control via Student's t test ($P < 0.05$).

associated increases in phosphorylation at multiple S6 phosphorylation sites and the LTD-associated increases in EF1A levels appears to be specific to mTOR inhibition because slices treated with the macrolide ascomycin, a compound structurally similar to rapamycin that does not inhibit mTOR, did not affect the DHPG-induced increase in S6 phosphorylation or EF1A expression (Fig. 4A and B). These findings are consistent with the notion that PI3K and mTOR are both required for the increases in S6 phosphorylation and translation of 5′TOP mRNAs associated with mGluR-LTD.

In addition to PI3K and mTOR, ERK is activated during DHPG-LTD (Fig. 1A and B) (4, 9). We therefore asked whether inhibition of MEK, the upstream kinase that phosphorylates and activates ERK, alters the LTD-induced increase in S6 phosphorylation and the increase in the levels of EF1A. We observed that the MEK inhibitor UO126 (20 μM, 1 h) blocked the LTD-induced increase in Ser235/Ser236 S6 phosphorylation and the increase in EF1A levels (Fig. 5A and B). Because p90RSK is activated by ERK and also can phosphorylate Ser235/Ser236 on S6, we also measured the Ser240/

Ser244 sites on S6 that have been reported to be specifically phosphorylated by S6Ks (36, 41). We found that mGluR-LTD was associated with increased levels of Ser240/Ser244 S6 phosphorylation that was blocked by the MEK inhibitor UO126 (Fig. 5A and B). We also observed that pretreatment of hippocampal slices with the MEK inhibitor SL327 (5 μM, 1 h), which is structurally distinct from UO126, had similar effects on Ser235/Ser236 S6 phosphorylation, Ser240/Ser244 S6 phosphorylation, and levels of EF1A (Fig. 5 legend). These results demonstrate that the unitary activation of each of the PI3K, mTOR, and ERK signaling pathways is required for DHPG-induced increases in S6 phosphorylation and EF1A synthesis.

mGluR-LTD is associated with increased S6K phosphorylation that is sensitive to inhibitors of PI3K, mTOR, and ERK. The PI3K, mTOR, and ERK signaling pathways are known to converge upon and activate S6Ks. Our observations that S6 phosphorylation at both the Ser235/Ser235 and Ser240/Ser244 sites was elevated during mGluR-LTD in an mTOR- and ERK-dependent manner prompted the hypothesis that S6K is selectively involved in mediating S6 phosphorylation and the concomitant elevation of EF1A. Therefore, we proceeded to examine whether increased S6K phosphorylation was associated with mGluR-LTD. S6K1 is abundant in the hippocampus (6, 49) and expressed largely in the cytoplasm, whereas S6K2 is expressed predominantly in the nucleus (24, 34, 36). Therefore, we concentrated our efforts on S6K1, for which specific antibodies are currently available. S6K1 is phosphorylated in a hierarchical manner, where the phosphorylation of the proline-rich portion of the kinase in the pseudocatalytic domain by mitogen-activated protein kinases, including ERK, is thought to "prime" the activation of the kinase. Subsequent phosphorylation of many sites by the upstream kinases phosphoinositide-dependent kinase 1, Akt, and mTOR follows this priming phosphorylation step (8). Notably, it has been reported that phosphorylation of the mTOR-sensitive site in the linker domain is most highly correlated with S6K activity (35). Therefore, we examined the phosphorylation of the ERK-dependent sites Thr421/Ser424 to measure putative priming of the kinase and the mTOR-dependent site Thr389 to measure activation of S6K1. We found that mGluR-LTD was associated with a significant increase in phosphorylation at the Thr421/Ser424 phosphorylation sites of the p70S6K isoform of S6K1 that was attenuated by the MEK inhibitor UO126 (Fig. 6A and B). We also observed that the phosphorylation of the Thr389 site of S6K1 was significantly increased following the application of DHPG (Fig. 6C and D). Pretreatment of the slices with either the PI3K inhibitor LY294002 or the mTOR inhibitor rapamycin blocked the DHPG-induced increase in S6K1 phosphorylation at the Thr389 site (Fig. 6C and D). The representative Western blot shown in Fig. 6A demonstrates that phosphorylation of p85S6K, the long isoform of S6K1, is likely to be regulated in a similar manner. Taken together, these findings suggest that increases in phosphorylation of S6K1 at both the Thr421/Ser424 and Thr389 sites may be required for subsequent increases in S6 phosphorylation and translation of 5′TOP mRNAs during mGluR-LTD.

mGluR-LTD is normally expressed in S6K1 knockout mice and abnormally enhanced in S6K2 and S6K1/S6K2 knockout mice. We next asked whether S6K knockout mice had a deficit
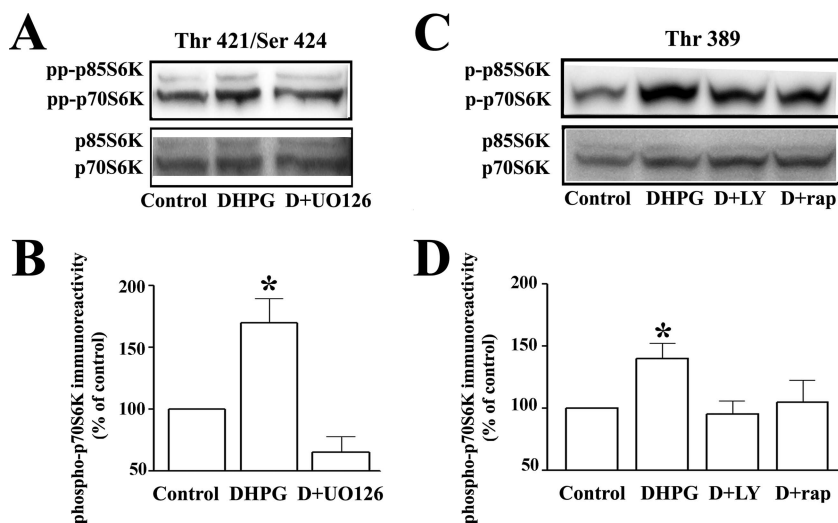
FIG. 6. DHPG induces phosphorylation of S6K that requires ERK, PI3K, and mTOR signaling pathways. Hippocampal slices were incubated in vehicle (0.01% DMSO or 0.01% methanol), UO126 (20 μM, 1 h), rapamycin (rap) (20 nM, 30 min), or LY294002 (LY) (50 μM, 30 min) and were then exposed to DHPG (50 μM) for 10 min in the presence of vehicle (control) or the respective antagonists. (A) Representative immunoreactivity for ERK-dependent phosphorylation of Thr421/Ser424 p70S6K, Thr444/Ser447 of p85S6K, and total p70/p85S6K in hippocampal CA1 homogenates. (B) Thr421/Ser424 phosphorylated p70S6K immunoreactivity was normalized to total p70S6K immunoreactivity. Values are means ± standard errors of the means. Percentages of control values for 421/424 p70S6K (pp-p70S6K) are as follows: with DHPG, 170% ± 21% ($n = 8$), and with DHPG plus UO126 (D+UO126), 65% ± 15% ($n = 4$) (data not shown: with DHPG plus LY, 70% ± 30% [$n = 4$]; with DHPG plus rap, 84% ± 28% [$n = 4$]). Phosphorylated p85S6K immunoreactivity could not be densitometrically quantified, as control-treated levels were not observed in most experiments. (C) Representative immunoreactivity for mTOR- and PI3K-dependent phosphorylation of Thr389 p70S6K, Thr412 p85S6K, and total p70/p85S6K in hippocampal CA1 homogenates. (D) Thr389 phosphorylated p70S6K immunoreactivity was normalized to total p70S6K immunoreactivity. Values are means ± standard errors of the means. Percentages of control values for Thr389 p70S6K (pp-p70S6K) are as follows: with DHPG, 140% ± 13% ($n = 8$); with DHPG plus rap (D+rap), 95% ± 13% ($n = 4$); and with DHPG plus LY (D+LY), 105% ± 21% ($n = 4$) (data not shown: with DHPG plus UO126, 124% ± 12% [$n = 4$]). *, statistical significance with vehicle-treated slices via Student's t test ($P \leq 0.05$).

in the expression of mGluR-LTD. Basic measures of synaptic function were examined in slices from both lines of knockout mice, and no differences in synaptic input/output curve or paired-pulse facilitation were observed compared to levels in slices from wild-type mice (2). In hippocampal slices from S6K1 knockout mice, the expression of mGluR-LTD, which is sensitive to protein synthesis inhibitors (15, 19), was still expressed (Fig. 7A and F). In contrast, we found that mGluR-LTD was enhanced in hippocampal slices from S6K2 knockout mice (Fig. 7B and F). This unexpected result led us to examine whether there was compensatory elevation of S6K1 in the S6K2 knockout mice that correlated with the enhanced LTD. We observed that S6K1 protein levels were similar in the hippocampi of wild-type and S6K2 knockout mice (Fig. 7C). This result does not exclude the possibility that S6K1 activity or its subcellular distribution is altered in S6K2-deficient mice. Therefore, we examined mGluR-LTD expression in S6K1/S6K2 double knockout mice to ascertain whether removal of both kinases resulted in a similar alteration in synaptic plasticity. In comparison to results for wild-type mice, we observed that mGluR-LTD also was enhanced in the S6K1/S6K2 double knockout mice (Fig. 7D and F). This result prompted us to determine whether mGluR-LTD in S6K2-deficient mice relies on the same fundamental requirement for de novo protein synthesis for expression. To address this, we measured the expression of mGluR-LTD in the presence of anisomycin in wild-type and S6K2-deficient mice. We found that anisomycin blocked the expression of LTD 60 to 80 min after induction in

wild-type mice. However, LTD expression persisted in S6K2 knockout mice up to 120 min following induction (Fig. 7E). Taken together these findings demonstrate that S6 kinases are not necessary for mGluR-LTD expression; however, removal of S6K2 results in abnormally enhanced protein synthesis-independent LTD.

LTD-induced phosphorylation of S6 is present in S6K1 and S6K2 knockout mice, but synthesis of EF1A is no longer coupled to mGluR activation. Because the expression of DHPG-induced mGluR-LTD was normal in S6K1 knockout mice and enhanced in S6K2 knockout mice, we next asked whether the LTD-associated increases in S6 phosphorylation and elevation of 5′TOP-encoded proteins were still present in slices from the S6K knockout mice. We found that in hippocampal slices from S6K1 knockout mice, expression of basal and LTD-induced increases in Ser235/Ser236 S6 and Ser240/Ser244 S6 phosphorylation remained comparable to that measured in slices from wild-type littermates (Fig. 8A, B, and C). In slices from the S6K2 knockout mice, basal levels of Ser235/Ser236 S6, but not Ser240/Ser244 S6, were modestly depressed compared to levels for wild-type mice (Fig. 8A, B, and C). However, the LTD-induced increases in Ser235/Ser236 S6 phosphorylation remained comparable to those in wild-type mice (Fig. 8A and B) and increases in Ser240/Ser244 S6 phosphorylation were similar to the LTD-induced increases in wild-type mice (Fig. 8A and C). Interestingly, the basal levels of EF1A were elevated in slices from both the S6K1 and S6K2 knockout
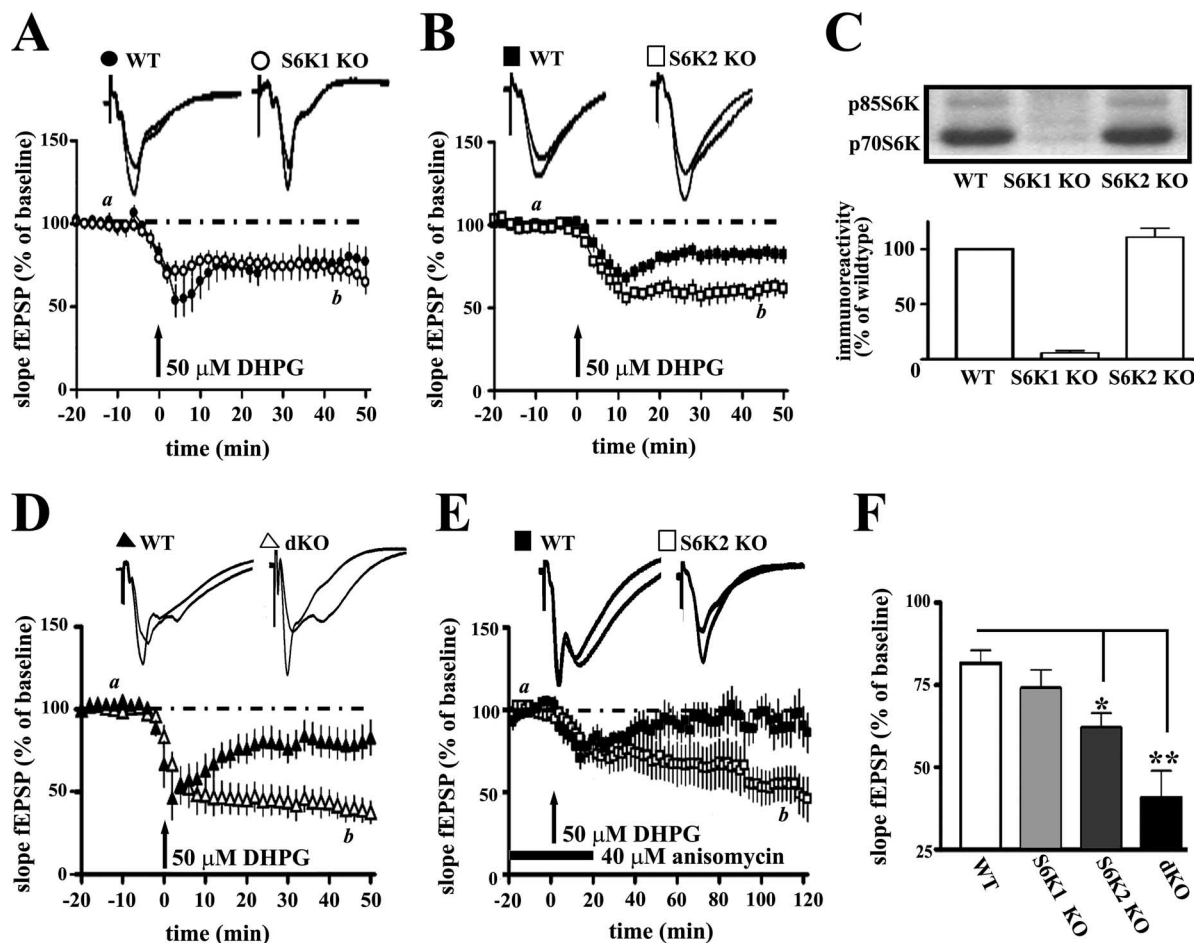
FIG. 7. mGluR-LTD in hippocampal slices from S6K knockout mice. (A, B, and D) mGluR-LTD was induced by incubation with DHPG (50 μM) for 10 min in slices from wild-type (WT), S6K1 knockout (S6K1 KO), S6K2 knockout (S6K2 KO), and S6K1/S6K2 double knockout (dKO) mice. For all recordings, at least 20 min of basal fEPSPs was recorded prior to LTD induction with DHPG. Representative fEPSPs 10 min before (a) and 45 min after (b) DHPG treatment in WT and KO slices are depicted on the top of each panel. (A) Ensemble averages for the initial slope of the fEPSP 20 min before, 10 min during, and 50 min after treatment with DHPG in WT and S6K1 KO hippocampal slices are shown at the bottom of the panel. For WT mice, eight slices were taken from seven animals, $t = 40$ to 50 min, and the fEPSP slope was $77\% \pm 9\%$ of baseline; for S6K1 KO mice, eight slices were taken from seven animals, $t = 40$ to 50 min, and the fEPSP slope was $65\% \pm 7\%$ of baseline. (B) Ensemble averages for the initial slope of the fEPSP 20 min before, 10 min during, and 50 min after treatment with DHPG in WT and S6K2 KO hippocampal slices are shown at the bottom of the panel. For WT mice, eight slices were taken from seven animals, $t = 40$ to 50 min, and the fEPSP slope was $82\% \pm 5\%$ of baseline; for S6K2 KO mice, eight slices were taken from seven animals, $t = 40$ to 50 min, and the fEPSP slope was $61\% \pm 5\%$ of baseline. (C) S6K1 levels in hippocampal homogenates from WT, S6K1 KO, and S6K2 KO mice. A representative Western blot is shown in the top panel, with the p85S6K and p70S6K isoforms of S6K1 indicated on the left. In the bottom panel, p70S6K1 immunoreactivity of each mutant animal was normalized to WT p70S6K1 immunoreactivity. (D) Ensemble averages for the initial slope of the fEPSP 20 min before, 10 min during, and 50 min after treatment with DHPG in WT and dKO hippocampal slices are shown. For WT mice, six slices were taken from three animals, $t = 40$ to 50 mine, and the fEPSP slope was $87\% \pm 7\%$ of baseline; for dKO mice, six slices were taken from three animals, $t = 40$ to 50 min, and the fEPSP slope was $41\% \pm 8\%$ of baseline. (E) mGluR-LTD was measured in slices from S6K2 KO or WT littermates in the presence of 40 μM anisomycin 1 h prior to, during, and 10 min after DHPG (50 μM for 10 min) treatment. Representative fEPSPs 10 min before (a) and 90 min after (b) DHPG treatment are depicted at the top of the panel. Ensemble averages for the initial slope of the fEPSP 20 min before, 10 min during, and 120 min after treatment with DHPG in WT and S6K2 KO hippocampal slices are shown at the bottom of the panel. For WT mice, five slices were taken from five animals, $t = 60$ to 80 min, and the fEPSP slope was $95\% \pm 9\%$ of baseline ($P > 0.1$ compared to $t = -20$ to 0 min); for S6K2 KO mice, eight slices were taken from five animals, $t = 60$ to 80 min, and the fEPSP slope was $66\% \pm 12\%$ of baseline ($P < 0.01$ compared to $t = -20$ to 0 min). (F) Comparison of LTD in WT, S6K1 KO, S6K2 KO, and dKO mice. Values were calculated 40 to 50 min after the start of DHPG treatment. For WT mice, the fEPSP slope was $82\% \pm 4\%$ of baseline (21 slices); for S6K1 KO mice, the fEPSP slope was $74\% \pm 6\%$ of baseline (10 slices); for S6K2 KO mice, the fEPSP slope was $62\% \pm 4\%$ of baseline (12 slices); and for dKO mice, the fEPSP slope was $41\% \pm 8\%$ of baseline (6 slices). Statistics were calculated with a one-way ANOVA, with a P value of <0.05 (∗) and a P value of <0.001 (∗∗) indicating significance compared to values for WT mice.

mice in comparison to levels for wild-type mice (Fig. 8A and D). Consequently, application of DHPG to these slices did not result in further elevation of EF1A levels (Fig. 8A and D). These findings indicate that, in slices from either S6K1 or S6K2 knockout mice, increases in S6 phosphorylation are still present following the induction of mGluR-LTD but that there is no longer mGluR-dependent synthesis of 5′ TOP-encoded proteins.
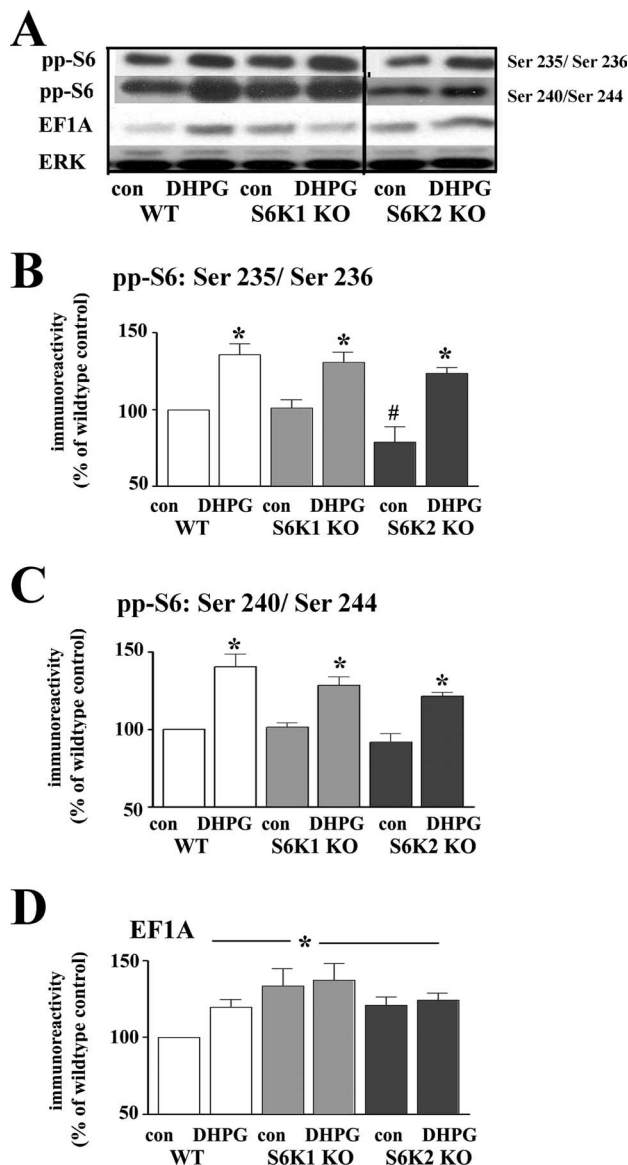
FIG. 8. mGluR-LTD in slices from S6K knockout mice is associated with normal phosphorylation of ribosomal protein S6 and abnormal expression of the 5′TOP-encoded protein EF1A. Hippocampal slices from wild-type (WT), S6K1 knockout (S6K1 KO), and S6K2 knockout (S6K2 KO) mice were incubated in DHPG (50 μM) for 10 min. (A) Representative Western blot from the same experiment within multiple gels for S6 phosphorylated at Ser235/Ser236 and Ser240/Ser244 (pp-S6), EF1A, and total ERK. (B to D) Immunoreactivity was normalized to total ERK immunoreactivity. Values are means ± standard errors of the means and are expressed as percentages of levels for the WT control (con). (B) Ser235/Ser236 pp-S6 values are as follows: for WT mice with DHPG, 136% ± 7% ($n = 5$); for S6K1 KO mice with control, 101% ± 5% ($n = 4$); for S6K1 KO mice with DHPG, 131% ± 6% ($n = 4$); for S6K2 KO mice with control, 79% ± 10% ($n = 3$); and for S6K2 KO mice with DHPG, 124% ± 4% ($n = 3$). (C) Ser240/Ser244 pp-S6 values are as follows: for WT mice with DHPG, 140% ± 8% ($n = 5$); for S6K1 KO mice with control, 101% ± 3% ($n = 4$); for S6K1 KO mice with DHPG, 128% ± 5% ($n = 4$); for S6K2 KO mice with control, 91% ± 5% ($n = 3$); and for S6K2 KO mice with DHPG, 121% ± 3% ($n = 3$). (D) EF1A values are as follows: for WT mice with DHPG, 120% ± 5% ($n = 5$); for S6K1 KO mice with control, 134% ± 11% ($n = 5$); for S6K1 KO mice with DHPG, 137% ± 11% ($n = 5$); for S6K2 KO mice with control, 121% ± 6% ($n = 3$); and for S6K2 KO mice with DHPG, 124% ± 5% ($n = 3$). *, statistical significance above control; #, statistical significance below WT control by Student's t test ($P < 0.05$).

DISCUSSION

Increased S6 phosphorylation and synthesis of EF1A are associated with mGluR-LTD. The precise consequence of S6 phosphorylation is not currently known and remains a question of intense debate (42). The supposition that S6 phosphorylation and protein synthesis via 5′TOP mRNA translation were correlated originally was proposed because both could be blocked with rapamycin. These events are now known to be independent of one another in nonneuronal cells (42). The recent generation of the S6 phosphorylation site mutant mouse has demonstrated that protein synthesis is not globally correlated with the state of S6 phosphorylation and/or 5′TOP mRNA translation (43). However, it was reported recently that S6 phosphorylation may improve the formation of the preinitiation complex necessary for synthesis of proteins in general (41). Given the current state of what is known about S6 phosphorylation and translation of 5′TOP mRNA, as well as the paucity of knowledge about these processes in neurons, we examined the levels of the 5′TOP-encoded protein EF1A in addition to the phosphorylation of multiples sites of S6 during mGluR-LTD. We found that phosphorylation of S6 is a good predictor of the selective enhancement in the total levels of EF1A and S6 during DHPG-induced mGluR-LTD. The LTD-associated increases in the levels of both EF1A and S6 could be blocked with anisomycin and were insensitive to proteasome inhibition, suggesting that EF1A and S6 are rapidly synthesized following the induction of mGluR-LTD. Our results are consistent with the DHPG-induced enhancement of phosphorylated S6 and EF1A synthesis previously measured in hippocampal dendrites (17) as well as the "all-or-none" activation of 5′TOP translation reported to occur in proliferating cells (28) and in dendrites during LTP (50). Our observations suggest that hippocampal neurons may become translationally competent in response to group I mGluR-mediated signal transduction events.

Interestingly, we found that the DHPG-induced increases in S6 phosphorylation and EF1A synthesis were localized predominantly in the soma of CA1 pyramidal neurons (Fig. 2). These findings resemble those from previous studies of mGluR-dependent increases in fragile X mental retardation protein levels in hippocampal neurons (1, 15). Taking into account that mGluR-LTD requires dendritic protein synthesis and that mGluR activation increases protein synthesis in synaptoneurosomes (12, 19), our results suggest the intriguing possibility that EFIA may be synthesized at synapses and transported back to the soma. Further experiments are required to determine whether this is the case.

DHPG-induced increases in S6K1 phosphorylation are PI3K, mTOR, and ERK dependent. A hierarchical model has been proposed (8) where phosphorylation via mitogen-activated protein kinases such as ERK is first necessary to "prime" S6K by relieving the autoinhibitory domain from the catalytic region of the kinase, allowing sequential phosphorylation of the kinase by multiple effectors, which include mTOR, Akt, PI3K, and phosphoinositide-dependent kinase 1. We found that mGluR-LTD was associated with robust phosphorylation of the priming sites Thr421/Ser424 of p70S6K1 that was blocked by the MEK inhibitor UO126 (Fig. 6A and B), which is consistent with a recent report of experiments conducted with synaptoneurosomes (33). We also detected an LTD-associated increase in the phosphorylation of the mTOR-sensitive

phosphorylation site (Thr389) that was abrogated by LY294002 and rapamycin (Fig. 6C and D). A similar increase in the phosphorylation of Thr389 on p70S6K1 following mGluR activation was recently reported by another group (40).

The difference in the magnitudes of the increase in phosphorylation of Thr421/Ser424 versus Thr389 on S6K1 during mGluR-LTD suggests differential regulation of signaling pathways upstream of these events. Notably, we observed that mTOR is tightly controlled during mGluR-LTD, because increased mTOR phosphorylation and activity were observed only immediately following DHPG treatment, quickly returning to the basal phosphorylation/activation state (Fig. 1A and B) (15). The brevity of the increase in mTOR activity and the relatively modest increase in Thr389 phosphorylation on S6K1 may be due to the tight regulation of the kinase by phosphatases and/or its numerous binding partners (44). In contrast, the increase in ERK2 activation during mGluR-LTD persists for 30 min after washout of DHPG (Fig. 1A and B). Taken together, our results support the notion that during mGluR-LTD the available pool of S6K1 that receives PI3K/mTOR-dependent modulation is altered due to the persistence of ERK-dependent priming of the kinase. Consistent with this notion, we found that inhibitors of both PI3K and mTOR decrease S6 phosphorylation and synthesis of EF1A (Fig. 3 and 4), demonstrating that activation of S6K1 during mGluR-LTD is correlated with PI3K-, mTOR-, and ERK-sensitive alterations in the kinase.

Our findings also demonstrate that inhibiting PI3K, mTOR, and ERK is unitarily sufficient to block the increase in S6 phosphorylation and enhanced levels of EF1A associated with mGluR-LTD. To our surprise, we did not observe a suppression of the LTD-associated increases in S6 phosphorylation and EF1A levels in either S6K1 or S6K2 knockout mice. We were unable to generate sufficient numbers of S6K1/S6K2 double knockout mice to determine conclusively whether S6Ks are absolutely required for the LTD-associated increases in S6 phosphorylation and levels of EF1A. Thus, it is still possible that in S6K1 knockout mice S6K2 phosphorylates S6 and that in S6K2 knockout mice S6K1 phosphorylates S6. Alternatively, it is possible that other signaling molecules mediate the phosphorylation of S6 and the levels of EF1A independently of S6Ks when they are absent. It has been reported previously that p90RSK regulates Ser235/Ser236 S6 phosphorylation and general levels of protein synthesis via the RAS/ERK pathway (41). In addition to regulating S6Ks directly, mTOR regulates 4E-binding protein to control cap-dependent translation during mGluR-LTD (4). Other regulators of 5′TOP mRNA translation that are PI3K dependent are suspected to exist (48). To delineate the specific contributions of these individual pathways requires further investigation.

Whether our observations of the phosphorylation state of S6K1 following induction of mGluR-LTD also reflect alterations in the sister kinase S6K2 remains unanswered. S6K1 and S6K2 contain similar phosphorylation sites and, some evidence suggests, similarities in responses to signaling pathways (8, 26, 27, 34). However, other studies suggest that there may be differential sensitivities of S6K1 and S6K2 to particular signaling inputs (24, 26, 51). Due to the relatively recent discovery of S6K2, phosphorylation state-specific tools are currently unavailable to assess whether ERK, PI3K, and/or mTOR differ-

entially alters S6K2 phosphorylation and function, and this remains a question of interest.

mGluR-LTD in S6K knockout mice. We hypothesized that removal of S6 kinases would result in the blockade of the protein synthesis-dependent phase of mGluR-LTD. We addressed this question with genetically engineered mice carrying a deletion of either the S6K1 or the S6K2 gene. Surprisingly, we observed that mGluR-LTD was expressed normally in the S6K1 knockout mice and enhanced in the S6K2 knockout mice (Fig. 7A and B). Compensatory changes in expression of each kinase are unlikely to be involved in this LTD phenotype, because we have observed that S6K1 is not upregulated in tissue from S6K2 knockout mice (Fig. 7C). Moreover, we have observed that enhanced LTD persists in S6K1/S6K2 knockout mice (Fig. 7D).

In addition to these observations, we found that LTD-induced S6 phosphorylation was intact in both the S6K1 and S6K2 knockout tissue (Fig. 8B). Similar observations have been reported for nonneuronal cells and suggest that neither S6K1 nor S6K2 is required for the induction of S6 phosphorylation or the synthesis of 5′TOP-encoded proteins (36, 46, 48). Also important to consider is that we were not able to measure LTD-associated increases in S6 phosphorylation and EF1A levels in S6K1/S6K2 double knockout mice. As mentioned earlier in the discussion, it is possible that S6 phosphorylation and EF1A synthesis are preserved in the single S6K null mice due to the residual activity of the remaining S6K or abnormal activity of other kinases, such as Akt (2, 16). Recent work has uncovered that S6K1 and S6K2 participate differently in the expression of learning, memory, and synaptic plasticity (2), suggesting that S6K1 and S6K2 have noncanonical functions. Recent progress has been made to determine the in vivo substrates of S6K1 and S6K2. To date, several substrates other than S6 (for a review, see reference 42) are known, including eukaryotic elongation factor 2 kinase and eukaryotic initiation factor 4B, which are both molecules that participate directly in the regulation of protein translation. In addition, known binding partners for S6Ks include neurabin (32) and eukaryotic initiation factor 3 (14). The RNA-binding protein SKAR has recently been identified as a unique substrate of S6K1 (38). Although no unique substrate of S6K2 has been identified to date, S6K2 does contain a proline-rich arm that may indicate unique regulation of kinase activity in comparison to S6K1 (11). Future studies of these potential effectors of S6Ks may uncover specific roles for these kinases in the expression of synaptic plasticity.

Interestingly, we observed that basal levels of Ser235/Ser236 S6 phosphorylation were low in the hippocampi of S6K2 knockout mice (Fig. 8). This finding is consistent with a previous report that S6K2 knockout mice have lower levels of S6 phosphorylation in both the cytosolic and nuclear fractions of cells than those observed from either wild-type or S6K1 knockout mice (36). In addition, we observed that the overall quantitative increase in Ser235/Ser236 S6 phosphorylation during mGluR-LTD in the S6K2 knockout mice was larger than that observed for either wild-type or S6K1 knockout mice (Fig. 8). In conjunction with our observation that mGluR-LTD was enhanced in S6K2 knockout mice (Fig. 7C and D), this leads to the intriguing possibility that the magnitude of Ser235/Ser236

S6 phosphorylation may directly correlate with the overall magnitude of LTD.

Although we observed that S6K is not necessary for either the expression of mGluR-LTD or the phosphorylation of S6, we did find that the levels of EF1A were exaggerated in the S6K knockout mice in comparison to levels in their wild-type littermates (Fig. 8); consequently, LTD-associated increases in EF1A levels were not observed in the S6K knockout mice (Fig. 8). EF1A levels are tightly regulated during development and decline rapidly during the early maturation of the brain (17, 21). Heightened expression of EF1A in conjunction with our observation that mGluR-LTD is no longer sensitive to anisomycin in the S6K knockout mice (Fig. 7E) suggests that S6Ks are involved in maintaining normal synaptic maturation. In this respect, S6K knockout mice are similar to *Fmr1* knockout mice, which also express anisomycin-insensitive LTD, abnormally high levels of synaptic proteins, and delayed synaptic development (5, 15, 29).

In the case of *Fmr1* knockout mice, fragile X mental retardation protein (FMRP), a negative regulator of protein synthesis, has been removed (23). We observed that S6K2 knockout mice and S6K1/S6K double knockout mice express enhanced LTD expression similar to that observed for *Fmr1* mutant mice (Fig. 7 and 8). Taking the similarity one step further, one could hypothesize that S6Ks repress the levels of proteins synthesized near synapses. Although this might appear to be a paradoxical hypothesis, it is well documented that general inhibition of global protein synthesis can improve the translational fidelity of the synapses by selecting for mRNAs that can be synthesized into protein when translational resources are limiting (23); this has been reported to occur at synapses during LTP but remains to be examined during mGluR-LTD (7).

Our findings indicate that the availability of proteins encoded by 5′TOP mRNAs is not compromised in S6K knockout mice, leaving open the possibility that translation of 5′TOP mRNAs is necessary for the expression of mGluR-LTD. Future examination of mice that specifically lack genes that are regulated via the 5′TOP structure is required to directly assess the relationship between translation of 5′TOP mRNAs and synaptic plasticity.

Dynamic translation of 5′TOP mRNAs may contribute to the expression of synaptic plasticity. We observed that the total levels of EF1A and S6 were enhanced following mGluR-LTD (Fig. 1A and C). EF1A is a crucial translation factor that mediates peptide elongation by promoting GTP-dependent binding of aminoacyl tRNA to the ribosome. Similar to our findings that EF1A synthesis is increased during mGluR-LTD, a form of protein synthesis-dependent plasticity, EF1A synthesis also has been reported to be elevated during protein synthesis-dependent LTP (49), and this elevation was accompanied by activation of S6K1 and additional synthesis of other 5′TOP mRNA-encoded proteins (50). Transport of EF1A mRNA was first identified in *Aplysia* neurites, where it was found to be synthesized during the maintenance phase of serotonin-induced long-term facilitation (10). In addition to the known function of EF1A as an elongation factor, noncanonical functions of EF1A are known to exist. One such role is for EF1A to promote the stabilization of actin monomers into the assembly of F-actin (25). Intriguingly, EF1A protein has been found to migrate toward activated synapses during in vivo LTP, an event that was blocked with the F-actin inhibitor latrunculin B (17). The involvement of EF1A in multiple forms of synaptic plasticity strongly suggests that EF1A is an essential molecule associated with the formation of long-term changes in synaptic strength.

We found that S6 phosphorylation and the total levels of S6 were elevated during mGluR-LTD (Fig. 1). These findings parallel previous findings in *Aplysia* synaptosome preparations treated with serotonin, a facsimile of protein synthesis-dependent long term-facilitation (22). Notably, increased S6 phosphorylation also has been observed after the induction of LTP and following training in a hippocampus-dependent memory task (20). Our findings, in conjunction with these previous studies, suggest that S6 phosphorylation is involved in multiple forms of synaptic plasticity and may be a signaling protein that indexes acquisition and expression of hippocampus-dependent memory.

Identification of proteins uniquely expressed during mGluR-LTD is important for the understanding of cognitive disorders. Renewed interest in identifying the proteins that are normally synthesized and expressed during mGluR-dependent signaling in the brain has arisen because mGluR-LTD is abnormally expressed in *Fmr1* knockout mice, a model of fragile X mental retardation (15, 18, 30). The abnormal expression of mGluR-LTD in this mouse model is due to the absence of FMRP, which is known to bind to and repress the translation of several mRNAs. In addition to the few proteins identified to be altered via mGluR-dependent signaling, we have identified EF1A and S6 as two proteins synthesized specifically in response to mGluR activation in hippocampal slices. Importantly, EF1A mRNA has previously been reported to bind to FMRP (47). Thus, alterations in the dynamic translation of 5′TOP mRNAs may play a pivotal role in the cognitive dysfunction associated with fragile X mental retardation.

REFERENCES

1. **Antar, L. N., R. Afroz, J. B. Dictenberg, R. C. Carroll, and G. J. Bassell.** 2004. Metabotropic glutamate receptor activation regulates fragile x mental retardation protein and FMR1 mRNA localization differentially in dendrites and at synapses. J. Neurosci. **24:**2648–2655.
2. **Antion, M. D., M. Merhav, C. A. Hoeffer, G. Reis, S. C. Kozma, G. Thomas, E. M. Schuman, K. Rosenblum, and E. Klann.** 2008. Removal of S6K1 and S6K2 leads to divergent alterations in learning, memory, and synaptic plasticity. Learn. Mem. **15:**29–38.
3. **Aschrafi, A., B. A. Cunningham, G. M. Edelman, and P. W. Vanderklish.** 2005. The fragile X mental retardation protein and group I metabotropic glutamate receptors regulate levels of mRNA granules in brain. Proc. Natl. Acad. Sci. USA **102:**2180–2185.
4. **Banko, J. L., L. Hou, F. Poulin, N. Sonenberg, and E. Klann.** 2006. Regulation of eukaryotic initiation factor 4E by converging signaling pathways during metabotropic glutamate receptor-dependent long-term depression. J. Neurosci. **26:**2167–2173.
5. **Bardoni, B., and J. L. Mandel.** 2002. Advances in understanding of fragile X pathogenesis and FMRP function, and in identification of X linked mental retardation genes. Curr. Opin. Genet. Dev. **12:**284–293.
6. **Cammalleri, M., R. Lutjens, F. Berton, A. R. King, C. Simpson, W. Francesconi, and P. P. Sanna.** 2003. Time-restricted role for dendritic activation of the mTOR-p70S6K pathway in the induction of late-phase long-term potentiation in the CA1. Proc. Natl. Acad. Sci. USA **100:**14368–14373.
7. **Costa-Mattioli, M., D. Gobert, H. Harding, B. Herdy, M. Azzi, M. Bruno, M.**

Bidinosti, C. Ben Mamou, E. Marcinkiewicz, M. Yoshida, H. Imataka, A. C. Cuello, N. Seidah, W. Sossin, J. C. Lacaille, D. Ron, K. Nader, and N. Sonenberg. 2005. Translational control of hippocampal synaptic plasticity and memory by the eIF2alpha kinase GCN2. Nature 436:1166–1173.

8. Dufner, A., and G. Thomas. 1999. Ribosomal S6 kinase signaling and the control of translation. Exp. Cell Res. 253:100–109.

9. Gallagher, S. M., C. A. Daly, M. F. Bear, and K. M. Huber. 2004. Extracellular signal-regulated protein kinase activation is required for metabotropic glutamate receptor-dependent long-term depression in hippocampal area CA1. J. Neurosci. 24:4859–4864.

10. Giustetto, M., A. N. Hegde, K. Si, A. Casadio, K. Inokuchi, W. Pei, E. R. Kandel, and J. H. Schwartz. 2003. Axonal transport of eukaryotic translation elongation factor 1alpha mRNA couples transcription in the nucleus to long-term facilitation at the synapse. Proc. Natl. Acad. Sci. USA 100:13680–13685.

11. Gout, I., T. Minami, K. Hara, Y. Tsujishita, V. Filonenko, M. D. Waterfield, and K. Yonezawa. 1998. Molecular cloning and characterization of a novel p70 S6 kinase, p70 S6 kinase beta containing a proline-rich region. J. Biol. Chem. 273:30061–30064.

12. Greenough, W. T., A. Y. Klintsova, S. A. Irwin, R. Galvez, K. E. Bates, and I. J. Weiler. 2001. Synaptic regulation of protein synthesis and the fragile X protein. Proc. Natl. Acad. Sci. USA 98:7101–7106.

13. Gressner, A. M., and I. G. Wool. 1974. The phosphorylation of liver ribosomal proteins in vivo. Evidence that only a single small subunit protein (S6) is phosphorylated. J. Biol. Chem. 249:6917–6925.

14. Holz, M. K., B. A. Ballif, S. P. Gygi, and J. Blenis. 2005. mTOR and S6K1 mediate assembly of the translation preinitiation complex through dynamic protein interchange and ordered phosphorylation events. Cell 123:569–580.

15. Hou, L., M. D. Antion, D. Hu, C. M. Spencer, R. Paylor, and E. Klann. 2006. Dynamic translational and proteasomal regulation of fragile X mental retardation protein controls mGluR-dependent long-term depression. Neuron 51:441–454.

16. Hou, L., and E. Klann. 2004. Activation of the phosphoinositide 3-kinase-Akt-mammalian target of rapamycin signaling pathway is required for metabotropic glutamate receptor-dependent long-term depression. J. Neurosci. 24:6352–6361.

17. Huang, F., J. K. Chotiner, and O. Steward. 2005. The mRNA for elongation factor 1alpha is localized in dendrites and translated in response to treatments that induce long-term depression. J. Neurosci. 25:7199–7209.

18. Huber, K. M., S. M. Gallagher, S. T. Warren, and M. F. Bear. 2002. Altered synaptic plasticity in a mouse model of fragile X mental retardation. Proc. Natl. Acad. Sci. USA 99:7746–7750.

19. Huber, K. M., M. S. Kayser, and M. F. Bear. 2000. Role for rapid dendritic protein synthesis in hippocampal mGluR-dependent long-term depression. Science 288:1254–1257.

20. Kelleher, R. J., III, A. Govindarajan, H. Y. Jung, H. Kang, and S. Tonegawa. 2004. Translational control by MAPK signaling in long-term synaptic plasticity and memory. Cell 116:467–479.

21. Khalyfa, A., D. Bourbeau, E. Chen, E. Petroulakis, J. Pan, S. Xu, and E. Wang. 2001. Characterization of elongation factor-1A (eEF1A-1) and eEF1A-2/S1 protein expression in normal and wasted mice. J. Biol. Chem. 276:22915–22922.

22. Khan, A., A. M. Pepio, and W. S. Sossin. 2001. Serotonin activates S6 kinase in a rapamycin-sensitive manner in Aplysia synaptosomes. J. Neurosci. 21:382–391.

23. Klann, E., M. D. Antion, J. L. Banko, and L. Hou. 2004. Synaptic plasticity and translation initiation. Learn. Mem. 11:365–372.

24. Lee-Fruman, K. K., C. J. Kuo, J. Lippincott, N. Terada, and J. Blenis. 1999. Characterization of S6K2, a novel kinase homologous to S6K1. Oncogene 18:5108–5114.

25. Liu, G., W. M. Grant, D. Persky, V. M. Latham, Jr., R. H. Singer, and J. Condeelis. 2002. Interactions of elongation factor 1alpha with F-actin and beta-actin mRNA: implications for anchoring mRNA in cell protrusions. Mol. Biol. Cell 13:579–592.

26. Martin, K. A., S. S. Schalm, C. Richardson, A. Romanelli, K. L. Keon, and J. Blenis. 2001. Regulation of ribosomal S6 kinase 2 by effectors of the phosphoinositide 3-kinase pathway. J. Biol. Chem. 276:7884–7891.

27. Martin, K. A., S. S. Schalm, A. Romanelli, K. L. Keon, and J. Blenis. 2001. Ribosomal S6 kinase 2 inhibition by a potent C-terminal repressor domain is relieved by mitogen-activated protein-extracellular signal-regulated kinase kinase-regulated phosphorylation. J. Biol. Chem. 276:7892–7898.

28. Meyuhas, O. 2000. Synthesis of the translational apparatus is regulated at the translational level. Eur. J. Biochem. 267:6321–6330.

29. Nosyreva, E. D., and K. M. Huber. 2005. Developmental switch in synaptic mechanisms of hippocampal metabotropic glutamate receptor-dependent long-term depression. J. Neurosci. 25:2992–3001.

30. Nosyreva, E. D., and K. M. Huber. 2006. Metabotropic receptor-dependent long-term depression persists in the absence of protein synthesis in the mouse model of fragile X syndrome. J. Neurophysiol. 95:3291–3295.

31. Nygard, O., and L. Nilsson. 1990. Translational dynamics. Interactions between the translational factors, tRNA and ribosomes during eukaryotic protein synthesis. Eur. J. Biochem. 191:1–17.

32. Oliver, C. J., R. T. Terry-Lorenzo, E. Elliott, W. A. Bloomer, S. Li, D. L. Brautigan, R. J. Colbran, and S. Shenolikar. 2002. Targeting protein phosphatase 1 (PP1) to the actin cytoskeleton: the neurabin I/PP1 complex regulates cell morphology. Mol. Cell. Biol. 22:4690–4701.

33. Page, G., F. A. Khidir, S. Pain, L. Barrier, B. Fauconneau, O. Guillard, A. Piriou, and J. Hugon. 2006. Group I metabotropic glutamate receptors activate the p70S6 kinase via both mammalian target of rapamycin (mTOR) and extracellular signal-regulated kinase (ERK 1/2) signaling pathways in rat striatal and hippocampal synaptoneurosomes. Neurochem. Int. 49:413–421.

34. Park, I. H., R. Bachmann, H. Shirazi, and J. Chen. 2002. Regulation of ribosomal S6 kinase 2 by mammalian target of rapamycin. J. Biol. Chem. 277:31423–31429.

35. Pearson, R. B., P. B. Dennis, J. W. Han, N. A. Williamson, S. C. Kozma, R. E. Wettenhall, and G. Thomas. 1995. The principal target of rapamycin-induced p70s6k inactivation is a novel phosphorylation site within a conserved hydrophobic domain. EMBO J. 14:5279–5287.

36. Pende, M., S. H. Um, V. Mieulet, M. Sticker, V. L. Goss, J. Mestan, M. Mueller, S. Fumagalli, S. C. Kozma, and G. Thomas. 2004. S6K1$^{-/-}$/S6K2$^{-/-}$ mice exhibit perinatal lethality and rapamycin-sensitive 5′-terminal oligopyrimidine mRNA translation and reveal a mitogen-activated protein kinase-dependent S6 kinase pathway. Mol. Cell. Biol. 24:3112–3124.

37. Raymond, C. R., V. L. Thompson, W. P. Tate, and W. C. Abraham. 2000. Metabotropic glutamate receptors trigger homosynaptic protein synthesis to prolong long-term potentiation. J. Neurosci. 20:969–976.

38. Richardson, C. J., M. Broenstrup, D. C. Fingar, K. Julich, B. A. Ballif, S. Gygi, and J. Blenis. 2004. SKAR is a specific target of S6 kinase 1 in cell growth control. Curr. Biol. 14:1540–1549.

39. Roberson, E. D., J. D. English, J. P. Adams, J. C. Selcher, C. Kondratick, and J. D. Sweatt. 1999. The mitogen-activated protein kinase cascade couples PKA and PKC to cAMP response element binding protein phosphorylation in area CA1 of hippocampus. J. Neurosci. 19:4337–4348.

40. Ronesi, J. A., and K. M. Huber. 2008. Homer interactions are necessary for metabotropic glutamate receptor-induced long-term depression and translational activation. J. Neurosci. 28:543–547.

41. Roux, P. P., D. Shahbazian, H. Vu, M. K. Holz, M. S. Cohen, J. Taunton, N. Sonenberg, and J. Blenis. 2007. RAS/ERK signaling promotes site-specific ribosomal protein S6 phosphorylation via RSK and stimulates cap-dependent translation. J. Biol. Chem. 282:14056–14064.

42. Ruvinsky, I., and O. Meyuhas. 2006. Ribosomal protein S6 phosphorylation: from protein synthesis to cell size. Trends Biochem. Sci. 31:342–348.

43. Ruvinsky, I., N. Sharon, T. Lerer, I. Cohen, M. Stolovich-Rain, T. Nir, Y. Dor, P. Zisman, and O. Meyuhas. 2005. Ribosomal protein S6 phosphorylation is a determinant of cell size and glucose homeostasis. Genes Dev. 19:2199–2211.

44. Sarbassov, D. D., S. M. Ali, and D. M. Sabatini. 2005. Growing roles for the mTOR pathway. Curr. Opin. Cell Biol. 17:596–603.

45. Shima, H., M. Pende, Y. Chen, S. Fumagalli, G. Thomas, and S. C. Kozma. 1998. Disruption of the p70(s6k)/p85(s6k) gene reveals a small mouse phenotype and a new functional S6 kinase. EMBO J. 17:6649–6659.

46. Stolovich, M., T. Lerer, Y. Bolkier, H. Cohen, and O. Meyuhas. 2005. Lithium can relieve translational repression of TOP mRNAs elicited by various blocks along the cell cycle in a glycogen synthase kinase-3- and S6-kinase-independent manner. J. Biol. Chem. 280:5336–5342.

47. Sung, Y. J., N. Dolzhanskaya, S. L. Nolin, T. Brown, J. R. Currie, and R. B. Denman. 2003. The fragile X mental retardation protein FMRP binds elongation factor 1A mRNA and negatively regulates its translation in vivo. J. Biol. Chem. 278:15669–15678.

48. Tang, H., E. Hornstein, M. Stolovich, G. Levy, M. Livingstone, D. Templeton, J. Avruch, and O. Meyuhas. 2001. Amino acid-induced translation of TOP mRNAs is fully dependent on phosphatidylinositol 3-kinase-mediated signaling, is partially inhibited by rapamycin, and is independent of S6K1 and rpS6 phosphorylation. Mol. Cell. Biol. 21:8671–8683.

49. Tsokas, P., E. A. Grace, P. Chan, T. Ma, S. C. Sealfon, R. Iyengar, E. M. Landau, and R. D. Blitzer. 2005. Local protein synthesis mediates a rapid increase in dendritic elongation factor 1A after induction of late long-term potentiation. J. Neurosci. 25:5833–5843.

50. Tsokas, P., T. Ma, R. Iyengar, E. M. Landau, and R. D. Blitzer. 2007. Mitogen-activated protein kinase upregulates the dendritic translation machinery in long-term potentiation by controlling the mammalian target of rapamycin pathway. J. Neurosci. 27:5885–5894.

51. Wang, L., I. Gout, and C. G. Proud. 2001. Cross-talk between the ERK and p70 S6 kinase (S6K) signaling pathways. MEK-dependent activation of S6K2 in cardiomyocytes. J. Biol. Chem. 276:32670–32677.

52. Weiler, I. J., and W. T. Greenough. 1993. Metabotropic glutamate receptors trigger postsynaptic protein synthesis. Proc. Natl. Acad. Sci. USA 90:7168–7171.

53. Wool, I. G. 1996. Mammalian ribosome: the structure and evolution of the proteins, p. 685–718. In J. W. B. Hershey and N. Sonenburg (ed.), Translational control. Cold Spring Harbor Laboratory Press, Cold Spring Harbor, NY.